ELSEVIER

26 July 1999

Physics Letters A 258 (1999) 359–366

PHYSICS LETTERS A

www.elsevier.nl/locate/physleta

Low-frequency voltage noise in SNS Josephson junctions arrays

M.C. Hernández [1]

Departamento de Física, Universidad Simón Bolívar, Apartado Postal 89000, Caracas 1080-A, Venezuela and Centro de Física, Instituto Venezolano de Investigaciones Científicas, Apartado Postal 21827, Caracas 1020-A, Venezuela

Received 7 January 1999; accepted 8 June 1999
Communicated by J. Flouquet

Abstract

We present low frequency voltage noise measurements in SNS Josephson junctions arrays both above and below the Kosterlitz–Thouless transition temperature. For zero applied magnetic field, the magnitude of the noise is found to have a maximum at T_{KT} and the spectral density $S_V(f)$ is a Lorentzian. When the array is fully frustrated the magnitude of $S_V(f)$ decreases with essentially no noise around T_{KT}. © 1999 Published by Elsevier Science B.V. All rights reserved.

PACS: 74.40.+k; 64.60.−i; 74.60.Ge; 74.50.+r
Keywords: Josephson junctions arrays; Kosterlitz–Thouless transition; Anomalous diffusion

Josephson arrays have proven to be quite useful in the study of phase transitions in two-dimensional systems. As a model system for the Kosterlitz–Thouless theory [1], arrays have allowed the study of both the thermodynamic and dynamic properties of low dimensional systems. These studies have shown that the KT theory and its generalization to Josephson arrays describe well most of the observed phenomena [2]. When a magnetic field is applied to these systems, arrays may also exhibit a variety of static and dynamic phenomena. Depending on the magnetic field, spin-glass and KT-like behavior have been found [3]. Dynamical properties, such as 'giant Shapiro steps' [4], were not only surprising, but also provided indirect information about the ground state of the system. Vortex dynamics in arrays has also been probed experimentally and the general picture of a vortex in the energy potential of the array describes well the experimental results. Fewer details are known about vortex diffusion and pinning of vortices in arrays, this is the case of ballistic vortices [5], where modeling shows ballistic motion to be limited by vortices losing energy to spin waves [6], in contrast with experiments. Low frequency phenomena are less well understood; very recent experimental studies and simulations [7,8] show a complex variety in the anomalous dynamical response, and the specific interactions that give rise this unexpected response is far to be clear.

In this paper, we further probe the dynamics of arrays through measurements of the low frequency voltage noise both above and below the Kosterlitz–Thouless transition temperature T_{KT}, in zero applied magnetic field ($\frac{\Phi}{\Phi_0}=0$), as well as in the fully frustrated case of $\frac{\Phi}{\Phi_0}=\frac{1}{2}$. We find that the noise

[1] E-mail: mcris@pion.ivic.ve

PII: S0375-9601(99)00382-5

increases sharply in magnitude and becoming Lorentzian as T_{KT} is approached. Below T_{KT}, the noise decreases in magnitude and becomes $\frac{1}{f}$-like at the lowest temperature measured. The characteristic times for the noise near the transition temperature are found to be of the order of milliseconds, inconsistent with the expected high frequency dynamics of vortices or the characteristic times for conventional vortex diffusion. We discuss the observed results in terms of different scaling regimes. Depending on characteristic length comparison, the spectra measured follows an anomalous diffusion of pairs, vortex pair generation and recombination at T_{KT}, or anomalous diffusion of free vortices.

Our samples consist of square arrays of 300 × 75 junctions of Nb–Au–Nb, made by electron-beam lithography to form cross-shaped islands of niobium on a continuous layer of gold; with a lattice constant of 10 μm a width on the arms of 1 μm and a separation of 0.5 μm between their tips. We first characterize the samples for the thermally induced vortex-unbinding transition through the measurement of the I–V characteristics, and the related power-law relationship $V(T) \propto I^{a(T)}$, as well as the jump of the exponent $a(T)$ predicted in the low current limit [9,10] from $a = 1$ at $T > T_{KT}$ to $a = 3$ at $T = T_{KT}$. The experimental setup for this characterization consists of a variable current source and a Keithley 148 nanovoltmeter, used in a fourth probe configuration. For temperature regulation between 10 K and 4.2 K, we used a Lake Shore Cryotronics temperature controller. Below 4.2 K we regulated the helium pressure, in order to avoid noise introduced by the controller.

A typical series of nonlinear I–V characteristic around T_{KT} at $\frac{\Phi}{\Phi_0} = 0$ is shown on Fig. 1(a); The solid line corresponds to a power law fit with an exponent of 3. For the sample presented in this paper we found, defining T_{KT} as the temperature for which $a(T) = 3$, $T_{KT} = (2.8 \pm 0.1)$ K. All the results presented here are similar to those measured in other samples. As a comparison is presented the corresponding series for the fully frustrated case in Fig. 1(b). Differences between both responses are evident. Even though each I–V characteristic can be fitted by a power-like dependence in each case, the discontinuity on the exponent is absent in the frustrated condition.

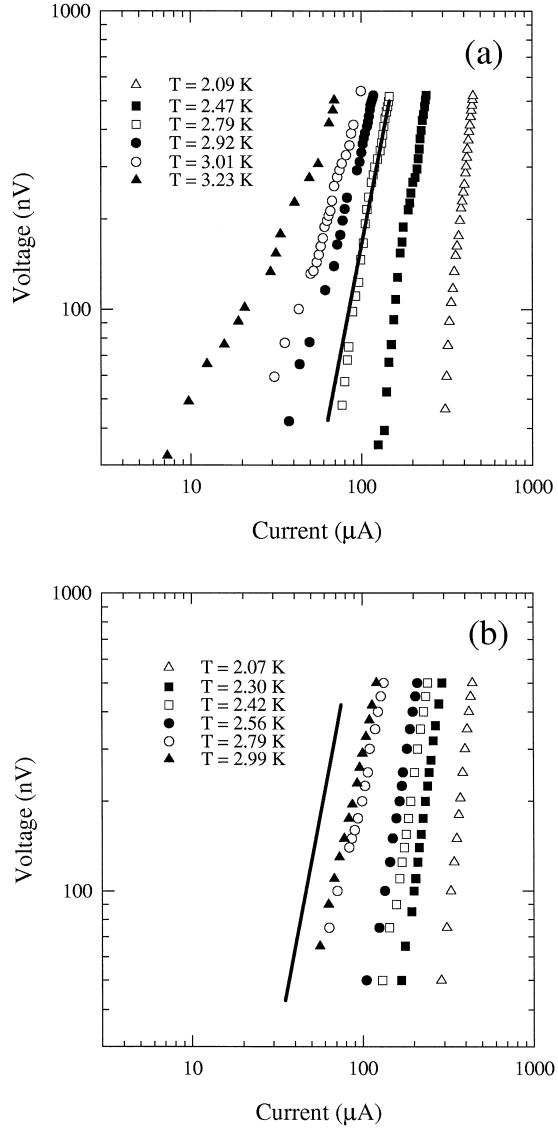

Fig. 1. Nonlinear I–V characteristic curves around T_{KT}. The solid line corresponds to $a = 3$. (a) Zero applied magnetic case, $\frac{\Phi}{\Phi_0} = 0$. (b) Fully frustrated case of $\frac{\Phi}{\Phi_0} = \frac{1}{2}$.

The experimental setup for the noise measurements is presented in Fig. 2. The voltage noise was characterized by applying a dc current to the sample and measuring the resulting voltage fluctuations after filtering. The dc voltage is eliminated through a blocking capacitor system (> 25000 μF), and further filtering is made with a home-made low-pass filter (cutoff frequency of 1 kHz). The resulting

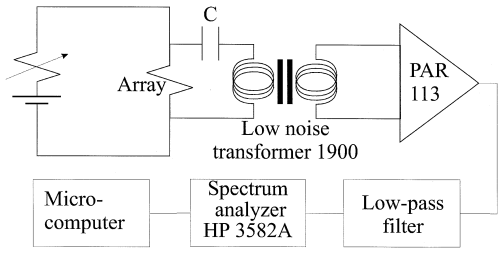

Fig. 2. The experimental setup for the noise measurements.

signal is amplified by 10^6, using a transformer and a low noise amplifier model PAR 190–113 system; the spectral density is measured with a HP 3582A spectrum analyzer. The noise setup resolution is limited by the instrumental noise, which is of the order of 10^{-20} $V^2/$ Hz

While the Kosterlitz–Thouless theory is strictly valid in the limit of no external perturbation, such as a magnetic external field or current, we perturb the array with a finite dc current, and thus have to choose whether the spectra should be compared at constant voltages or currents. While the results in both cases are qualitatively similar near and below T_{KT}, the highly nonlinear I–V characteristics make comparisons at fixed current inadequate. Due to the fact that the driven current through the array by fixing the voltage has a much lower value above T_{KT} than the corresponding at a fixed current. As a consequence, by fixing the voltage the effects of current induced free vortices are minimized. Thus, we made first a characterization at a fixed voltage, the lowest voltage permitted by our sensitivity, which minimizes the undesirable effects of pair-breaking. After that we studied the perturbation of the Kosterlitz–Thouless transition by increasing the applied current at T_{KT}.

Fig. 3 shows a typical series of spectra for $S_V(f)$ as a function of frequency, at a voltage of 50 nV, both above and below $T_{KT} =$ 2.8 K in both zero applied magnetic field and full frustration. Note the remarkable difference in the data depending on whether the system is frustrated or not. Near the transition for $\frac{\Phi}{\Phi_0} = \frac{1}{2}$, the spectral density is always at least two orders of magnitude lower than for $\frac{\Phi}{\Phi_0} = 0$, and all the spectra for $\frac{\Phi}{\Phi_0} = \frac{1}{2}$ above and below T_{KT} are near the limit of sensitivity of our experimental system (which is approximately 10^{-20} $V^2/$ Hz). Only at the lowest temperature shown in Fig. 3 is there a measurable signal for $\frac{\Phi}{\Phi_0} = \frac{1}{2}$.

For $\frac{\Phi}{\Phi_0} = 0$, the voltage noise in Fig. 3 shows three different regimes. First, above the Kosterlitz–Thouless transition temperature T_{KT}, the spectrum is $\frac{1}{f}$-like (open triangles). Second, very close to T_{KT}, the noise begins to rise, changing from $\frac{1}{f}$-like to a Lorentzian (open circles). Finally, as the sample is cooled below the transition temperature the magnitude of the noise decreases and the Lorentzian spectrum slowly changes back to a $\frac{1}{f}$-like spectrum (filled triangles). When the temperature approaches T_{KT} from below, the shape of the voltage noise changes and at T_{KT}, the spectral density is a Lorentzian (curve solid line). This clearly suggests that the noise increase at T_{KT} is a consequence of vortex–antivortex unbinding.

In Fig. 4 we show in detail how the noise magnitude increases at T_{KT} for three different frequencies. The maximum magnitude in the noise is found at $T = 2.8$ K, consistent with the value of T_{KT} deter-

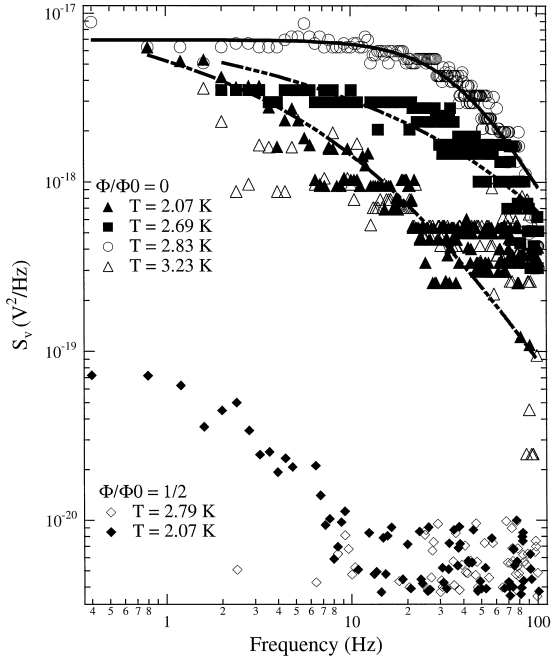

Fig. 3. Spectral density versus frequency at 50 nV above and below T_{KT}, for zero applied magnetic field and full frustration. Solid line corresponds to a Lorentzial fit and dashed ones correspond to Eq. (4) fit.

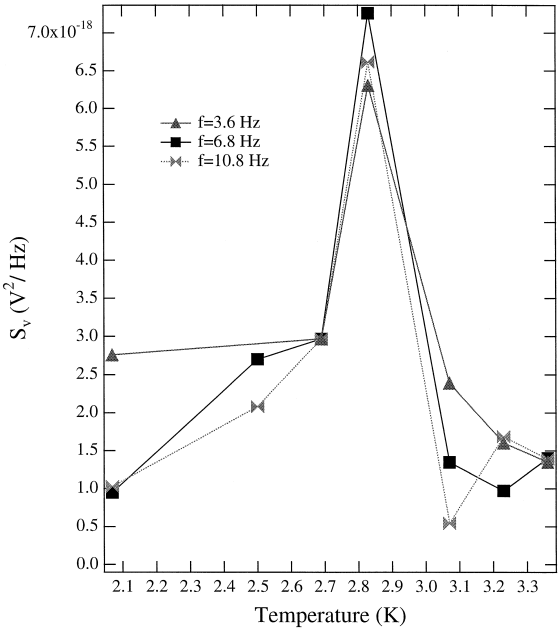

Fig. 4. Spectral density versus temperature for three different frequencies.

mined from the I–V characteristics, within experimental error. The fact that this maximum in the noise spectrum coincides with the point where the sample becomes superconducting, suggests that the noise is due to temperature fluctuations. However, if this were the case, there should also be a similar peak when $\frac{\Phi}{\Phi_0} = \frac{1}{2}$, which is not observed. Furthermore, comparison of the detailed temperature dependence of our experiments with the dependence expected from temperature fluctuation model [11], $S_V/V^2 \propto R^{-1}\frac{dR}{dT}$, is inconsistent with this possibility, due to the fact that this model predicts a divergence of the spectral density below T_{KT} which is not observed in our results. Similar results to those shown in Fig. 4 have been published by Voss et al. [12] in high-resistivity granular films of aluminum and tin, near the superconducting transition. However, the peak in the noise observed by Voss et al., which was interpreted as a consequence of free vortices induced by the applied current, *increased* with the dc current and scaled with it, which is characteristic of flux-flow resistance noise, rather than decrease with dc current as shown in Fig. 5.

In Fig. 5 we prove that the observed Lorentzian spectra measured at T_{KT} is indeed related to the presence of vortex pairs in the system. At the lowest current used, the noise spectrum is a Lorentzian (Fig. 3), but as the dc current level is increased (Fig. 5), the magnitude of the noise decreases with essentially no difference between this 'high current' spectra at T_{KT}, and those obtained at a higher temperature, shown in Fig. 3. Thus, whatever the physical origin of the voltage fluctuations is, finite currents reduce and even completely change them, conclusively showing that the voltage fluctuations observed are related to pair vortex–antivortex dynamics.

The KT transition is strictly valid in the thermodynamic limit when the system is infinite and the applied current is zero. Vortex dynamics in two dimensions shows an anomalous response characterized at low frequencies with a logarithmic divergence of the conductivity, which seems to be an intrinsic property on such systems. In weakly perturbed finite systems the dynamical behavior around KT transition is strongly controlled by the length scales that dominate the problem. Following a recent theoretical analysis [13], is necessary to consider

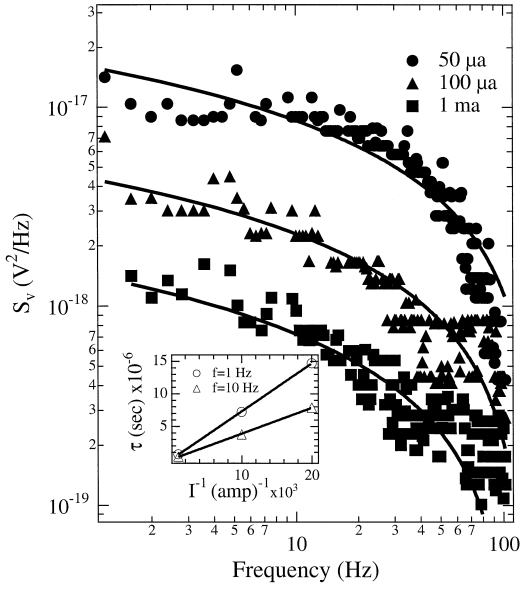

Fig. 5. Spectral density versus frequency at T_{KT} for three different applied currents. Solid curves correspond to the fit using Eq. (5). The inset shows the dependence τ vs $\frac{1}{I}$ and its linear fit for two frequencies.

current and finite size effects, besides the thermal correlation length $\xi(T)$, in order to improve the physical comprehension of some observed results. Due to our noise characterization, we have to consider finite current effects introducing the current length ξ_I, defined as the maximum size of bound vortex pairs in the presence of a current I. The finite size effect is taken into account with the linear extent of the array L. The dynamical vortex response [14] is driven by the dynamical length scale $\lambda_f = \sqrt{\frac{D}{2\pi f}}$ where D is the vortex diffusion constant and f is the frequency. This length is interpreted as a measure of the length scale over which the time average of the pair correlation length is destroyed due to dynamics. Below T_{KT} the correlation length $\xi(T)$ diverges, and the scales of the system are dominated by ξ_I, L and λ_f. In our experimental setup, the constant voltage condition below T_{KT}, guarantees the relation $\xi_I > L$ and the characteristic lengths L and λ_f become the relevant scales in this regime. Therefore, the vortex response is driven by the finite size and pairs dynamical response. To interpret voltage noise spectra below the transition, we use the Minnhagen phenomenological model [15] extensively utilized to describe bound vortex–antivortex response [7]. The voltage noise measures the complex impedance, which is a reflect of the dynamical properties of the vortex system. Using the Coulomb gas analogy with vortices, the imaginary contribution to the dielectric constant associated with the dissipative part of the vortex response is:

$$\mathrm{Im}\left[\frac{1}{\varepsilon(f)}\right] = \frac{4(Y-C)\ln(Y)}{\pi(1-Y^2)}, \tag{1}$$

with

$$Y = \frac{\omega_0}{2\pi f} \tag{2}$$

and

$$C = \frac{D}{L^2 2\pi f}. \tag{3}$$

The term $\omega_0(T)$ is a temperature dependent characteristic frequency, and is related to the screening length of the vortex system. The parameter C considers finite size effects due to the contribution of L (for infinite systems $C = 0$). In the case of no applied magnetic field, the voltage noise is related to the imaginary part of the dielectric constant by:

$$S_V(f) = -\frac{4k_{\mathrm{B}}L_K e^2 T}{\hbar^2 \pi f}\mathrm{Im}\left[\frac{1}{\varepsilon(f)}\right] = \frac{32K_{\mathrm{B}}L_K e^2 T}{\hbar^2\pi}\frac{\left(\omega_0 - DL^{-2}\right)}{\left(\omega_0^2 - (2\pi f)^2\right)}\ln\left(\frac{\omega_0}{2\pi f}\right). \tag{4}$$

In order to investigate the temperature dependence of the voltage fluctuations below T_{KT}, we use for the kinetic inductance the Ginzburg–Landau result $L_K \propto 1 - \frac{T}{T_{c0}}$, where T_{c0} is the Ginzburg–Landau temperature. Using Eq. (4) to fit the spectra below the transition we obtain the characteristic frequency and the diffusion constant at each temperature in this regime (dashed lines on Fig. 3 correspond to Eq. (4) fit). The Fig. 6 shows the temperature dependence of ω_0. According to Minnhagen's description, ω_0 is a monotonic increasing function of temperature, proportional to the screening length of the vortex system, and consequently proportional to the resistance. This behavior suggests a dependence of the form $V \propto I$, in accordance with the linear behavior predicted below T_{KT} in the low current limit [13] when $\xi_I > L$. This linear resistance below KT-transition is supported by the temperature dependence [16] $\ln\omega_0 \propto \left(\frac{\hbar}{2e}I_c(T)\right)/k_{\mathrm{B}}T = \frac{1}{\tau}$ shown in Fig. 6. The diffusion constant found from the fits presents a weak increase with temperature for values within the range ($0.14\ \mathrm{cm}^2/\mathrm{s} < D < 0.26\ \mathrm{cm}^2/\mathrm{s}$); for this values the dynamical length can be calculated and is found to be $0.01\ \mathrm{cm} < \lambda_f < 0.2\ \mathrm{cm}$. The relationship between the length scales is $\lambda_f < L$ ($L = 0.3$ cm), which corresponds to the validity range of the Minnhagen's model [14].

At T_{KT} the Eq. (4) can not fit the measured spectrum and the later description fails. This behavior would be explained due to the increase of λ_f as the diffusion constant is increased and to the crossover to comparable length scales ($\lambda_f \approx L$). We found a Lorentzian frequency dependence typically appearing in processes in which there is a single characteristic time. We find from fitting all our data near T_{KT} that the average characteristic time is $\tau =$

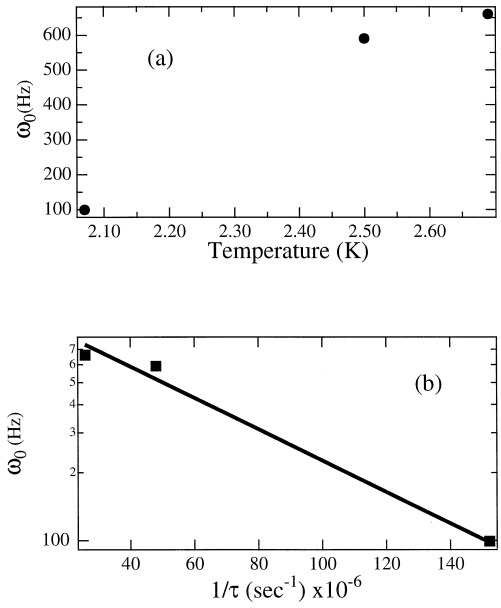

Fig. 6. (a) corresponds to The temperature dependence of ω_0, and (b) shows the ω_0 versus $\frac{1}{\tau}$ dependence, the solid line corresponds to the function $\ln\omega_0$ versus $\frac{1}{\tau}$.

(4 ± 3) ms. This time is relatively large in comparison with characteristic times for typical processes in superconducting films [17], such as the characteristic time for laser pulsed-induced vortex motion ($\tau < 10^{-8}$ s), or free vortex diffusion in high-resistance granular films ($\tau < 10^{-5}$ s). To explain the contribution of pair dissociation to the noise at T_{KT}, we consider a generation-recombination model similar to that used to explain voltage noise in strongly extrinsic semiconductors [18]. In analogy with this model, we associate a lifetime with the mechanisms of generation of free vortices and that of recombination of vortex–antivortex [19] pairs. In this case, the recombination rate r is proportional to the square of the free vortex density $r = \alpha n_f^2(I)$, and the generation rate g can be modeled assuming classical escape over a potential barrier $g = \beta\exp(-U_0/k_B T)$, where α and β are constants, n_f is the free vortex density and U_0 is the height of the potential barrier.

The characteristic time of the generation-recombination of vortices will be given by the rate equation: $\frac{1}{\tau_r} = \frac{dr}{dn_f} - \frac{dg}{dn_f}$, and only the free vortex density contribute to the characteristic time τ_r. An estimate of this time using the Halperin and Nelson continuum theory [9] gives: $\tau_r = 1/(8\pi\mu k_B T n_f) = 1/(8\pi D n_f)$. The density of free vortices in real systems is different than zero above the ground state and scales at T_{KT} as $n_f = L^{-2}$ whereas the constant diffusion can be expressed in terms of the scaling length as $D = 2\pi f\lambda_f^2$. All this leads to the equation for the characteristic time: $\tau_r = \left(L/\lambda_f\right)^2 1/(16\pi^2 f)$. Assuming that at T_{KT} the characteristic lengths are comparable ($\frac{L}{\lambda_f} \approx 1$), and that de correlated fluctuations are within the range $1 < f < 10$ Hz, the characteristic time ranges within the interval $0.6 < \tau_r < 6$ msec, in very good agreement with our experimental results. This Lorentzian dependence might be interpreted as a Drude behavior, associated with free vortex diffusion at T_{KT}, but noise response found at the transition as the current is increased, as well as the vanish signal for $\frac{\Phi}{\Phi_0} = \frac{1}{2}$ around T_{KT}, allows us to affirm that this is a consequence of vortex pair unbinding.

If the current is now increased through to the sample at T_{KT}, $\xi_I \propto I^{-1}$ becomes the characteristic scale and a different mechanism drives the dynamical response as free vortex motion across the sample increases. A free vortex reaching the edge of the sample will generate a voltage pulse of height $2\pi\Phi_o/\tau$ and width τ, where τ the transit time needed to cross the sample. While one might expect this process to be described by classical diffusion, direct measurement of the dielectric constant in arrays [20] show that free vortex diffusion becomes anomalously slow at low frequencies. This is apparently due to the coupling of the vortices to the spin wave excitations of the array, thus indicating that this is a general property of a 2D superfluid system. The detailed characterization of the dielectric constant leads to a Drude-like expression where the conductivity is frequency-dependent, resulting a power spectrum of the form:

$$S_V(f) = \frac{A\tau(f)}{1 + (\pi f\tau(f))^2}, \tag{5}$$

with

$$\tau(f) = \frac{\Phi_o W^2}{R_0 a_0^2 I}\frac{1}{\mu\left(\frac{f_0}{f}\right)} = \frac{\Phi_o W^2}{R_0 a_0^2 I}\frac{2}{\pi}\ln\left(\frac{f_0}{f}\right), \tag{6}$$

where R_0 is the normal resistance, a_0 is the lattice spacing, W is the transversal length ($W = 75a_0$), and f_0 is a characteristic frequency. While Drude-like classical diffusion would yield times that are too short to explain our results, the logarithmic dependence of the vortex mobility with frequency gives rise to an anomalous vortex diffusion explained as a sluggish vortex motion and observed at low frequencies in similar systems. This model yields characteristic times which are in line with our experiments. We can use the results of anomalous diffusion to calculate the power spectrum of the fluctuations and compare it to that measured in our samples in the presence of a current, with A and f_0 as fitting parameters. Fig. 5 presents the spectral density at T_{KT} for different currents and its respective fit using Eq. (5). The agreement between the experimental curve and the fit is excellent. From the characteristic frequencies f_0 found for each curve ($f_0 > f$), we can also calculate τ as a function of the frequency and verify experimentally the relationship $\tau \propto I^{-1}$. The inset in Fig. 5 presents the characteristic time as a function of $\frac{1}{I}$ at two frequencies and its corresponding linear fitting. The agreement between the two is quite good, demonstrating the $\frac{1}{I}$ dependence predicted by the model. The current dependence of the characteristic times as well as the frequency range of the voltage fluctuations observed in this free vortex regime provides strong evidence for anomalous slow diffusion of free vortices at large time scales.

While anomalous diffusion is characteristic of disordered systems, it is unlikely that it can explain our results. The question still remains as to the origin of the slowdown of vortices in these systems. Well below T_{KT} vortices interact in different ways with the pinning potential due to the lattice of junctions, depending on frustration. It is known [21] that the pinning energy for $\frac{\Phi}{\Phi_0} = \frac{1}{2}$, is much higher than for $\frac{\Phi}{\Phi_0} = 0$; this interaction with the lattice explains the dramatic difference observed in the voltage fluctuations well below the Kosterlitz–Thouless transition for zero or full frustration, and give us additional evidence to discard any pinning interaction in explain the results for $\frac{\Phi}{\Phi_0} = 0$. Furthermore, just at T_{KT} it is well known that pinning interaction with the lattice is less important [10]. This evidence leads us to exclude any pinning mechanism as an explanation of the observed sluggish vortex motion. Due to the temperature range used in our experiments, we also discard any quantum effect. This anomalous diffusive vortex motion found both above and below T_{KT} appears to be an intrinsic dynamic property in two dimensions. As a possible mechanism of low vortex mobility at low frequencies, is suggested around T_{KT} an interaction between free vortices and thermally induced bound pairs or vortices coupling with spin waves. Even though simulations in this regime have been made on the underdamped case, comparison with experiments is yet unclear. In the overdamped regime, some kind of dynamical vortex mass may generate spin waves by losing 'kinetic energy', resulting in a sluggish vortex mobility. Comparing our results in the region $T \geq T_{KT}$, with those presented by Shaw et al. [8], a clear difference is observed in the form of the spectra. Dynamic simulations using time dependent Ginzburg–Landau in 2D *xy* models [7], demonstrate that the variation of the function $\mathrm{Im}\left[\frac{1}{\varepsilon(f)}\right]$ with the density of vortex around T_{KT} can explain such a difference. Our measures correspond to the case of low densities of thermally created vortices, whereas the results of Shaw et al. [8] correspond to a higher density case. Different simulated flux noise results are found, using the phenomenological Minnhagen picture above the transition [22], or at T_{KT} in a high vortex density limit [23], however, differences are not surprising if we consider that the observed results presented here are an indication of finite current and size effects, that the simulated results do not take into account.

As the extensive and recent literature shows, the dynamical vortex response around T_{KT} even without an applied magnetic field, is more complex than expected. Effects such as coupling between free and pair vortex [24], spin-waves and vortices interactions, and more recently finite size and current effects must be considered in order to understand the observed phenomena.

In conclusion, the presented low voltage noise measurements on arrays of Josephson junctions show unexpected and novel characteristics. Below the Kosterlitz–Thouless transition finite size scaling as well as anomalous pair diffusion appears to describe the observed voltage fluctuations. The spectra found at the transition indicates the existence of an unique characteristic time associated with vortex–antivortex pair unbinding, and this feature is explained in terms

of the generation-recombination model. Above this transition, the scaling of voltage noise with current strongly supports this analysis, and the relatively high characteristic times observed above T_{KT} are well explained in terms of an anomalous low free vortex diffusion at zero frustration.

Acknowledgements

We acknowledge D.B. Mast for the sample preparation. We are also grateful to J.M. Aponte (†), L.E. Guerrero, C.J. Lobb, R. Newrock, and M. Octavio for the stimulating discussions and critical reading of the manuscript.

References

[1] J.M. Kosterlitz, D.J. Thouless, J. Phys. C 5 (1972) L124; 6 (1973) 1181; V.L. Berezinskii, Sov. Phys. JETP 34 (1972) 610.
[2] D.W. Abraham, C.J. Lobb, M. Tinkham, T.M. Klapwijk, Phys. Rev. B 26 (1982) 5268.
[3] S. Teitel, C. Jayaprakash, Phys. Rev. B 27 (1983) 598; M.Y. Choi, D. Stroud, Phys. Rev. B 32 (1985) 5773.
[4] S.P. Benz, M.S. Rzchowski, M. Tinkham, C.J. Lobb, Phys. Rev. Lett. 64 (1990) 693.
[5] H.S.J. Van der Zant, F.C. Fritschy, T.P. Orlando, E. Mooij, Europhys. Lett. 18 (1992) 343.
[6] U. Geigenmuller, C.J. Lobb, C.B. Whan, Phys. Rev. B 47 (1993) 348.
[7] A. Jonsson, P. Minnhagen, Phys. Rev. B 55 (1997) 9035.
[8] T.J. Shaw, M.J. Ferrari, L.L. Sohn, D.L. Lee, M. Tinkham, J. Clark, Phys. Rev. Lett. 76 (1996) 2551.
[9] B.I. Halperin, D.R. Nelson, J. Low Temp. Phys. 36 (1979) 599.
[10] C.J. Lobb, D.W. Abraham, M. Tinkham, Phys. Rev. B 27 (1983) 150.
[11] R.F. Voss, J. Clarke, Phys. Rev. B 13 (1976) 556.
[12] R.F. Voss, C.M. Knoedler, P.M. Horn, Phys. Rev. Lett. 45 (1980) 1523.
[13] M.V. Simkin, J.M. Kosterlitz, Phys. Rev. B 55 (1997) 11646.
[14] M. Capezzali, H. Beck, S.R. Shenoy, Phys. Rev. Lett. 78 (1997) 523.
[15] P. Minnhagen, Rev. Mod. Phys. 59 (1987) 1001.
[16] H.S.J. Van der Zant, H.A. Rijken, J.E. Mooij, J. Low Temp. Phys. 79 (1990) 289.
[17] J.E. Mooij, NATO Advances in Superconductivity, Erica, Italy, 1982.
[18] Van der Ziel, Noise: Sources, Characterization, Measurement, Prentice Hall, 1970.
[19] A.M. Kadin, K. Epstein, A.M. Goldman, Phys. Rev. B 27 (1983) 6691.
[20] R. Theron, J.B. Simond, Ch. Leemann, H. Beck, P. Martinoli, P. Minnhagen, Phys. Rev. Lett. 71 (1993) 1246.
[21] M.S. Rzchowski, S.P. Benz, M. Tinkham, C.J. Lobb, Phys. Rev. B 42 (1990) 2041.
[22] J. Houlrik, A. Jonsson, P. Minnhagen, Phys. Rev. B 50 (1994) 3953.
[23] A. Jonsson, P. Minnhagen, Phys. Rev. Lett. 73 (1994) 3576.
[24] A. Jonsson, P. Minnhagen, Physica C 277 (1997) 161.